JOURNAL OF SOLID STATE CHEMISTRY 83, 207–213 (1989)

Splitting of High-Temperature X-Ray Diffraction Profiles during the PbO Tetragonal ⇄ Orthorhombic Phase Transformation

J. R. SCHOONOVER, T. L. GROY, AND S. H. LIN

Department of Chemistry, Arizona State University, Tempe, Arizona 85287-1604

Received March 7, 1989

In situ high-temperature X-ray diffraction of the PbO tetragonal ⇄ orthorhombic transformation shows the profiles of each phase split into several peaks. The intensities are a function of time and the average position is that of the undistorted profile. A unit cell distortion extends throughout a diffraction domain, and when averaged over the specimen there is no global change in symmetry. The splitting is not evident in quenched specimens. There is uncertainty whether the splitting is of the transformation mechanism or from the presence of ordered defects accompanying the transformation.

1. Introduction

There are at least two phases of PbO. The low-temperature red phase is made up of sheets of PbO_4 pyramids perpendicular to $[001]_t$, and the high-temperature yellow orthorhombic phase is composed of PbO chains along $[010]_0$. The tetragonal → orthorhombic phase transformation occurs at about 593°C. It is reversible, although the yellow phase is metastable at room temperature and may persist for years. The interface between the two phases is continuous rather than sharp (*1*). The transformation is reconstructive and interfacially controlled. The transformation is topotactic with $(001)_t \| (001)_0$ and $[110]_t \| [100]_0$ (*1*). The topotactic plane has been confirmed by us through texture studies (*2*). The mechanism was postulated by Söderquest and Dickens (*1*) to be a rotation of oxygen atoms about the lead atoms with bond length distortions accompanied by small displacements of the lead. Dickens reports a 2% expansion along $[100]_0$, an 18% expansion along $[101]_0$, and a 13% contraction along $[001]_0$. The lead atoms move 0.17 Å normal to the tetragonal sheets and are pushed apart 0.44 Å along $[010]_0$.

Nucleation and growth kinetics by X-ray diffraction of quenched specimens at 1 atm have been reported (*3*). The transformation curves shown appear isothermal and follow avrami kinetics. The pressure-induced transformation has been reported as being martinsitic (*4*). Apart from the above work, the transformation is not well characterized.

We have applied high-temperature X-ray diffraction to the tetragonal ⇄ orthorhom-

0022-4596/89 $3.00

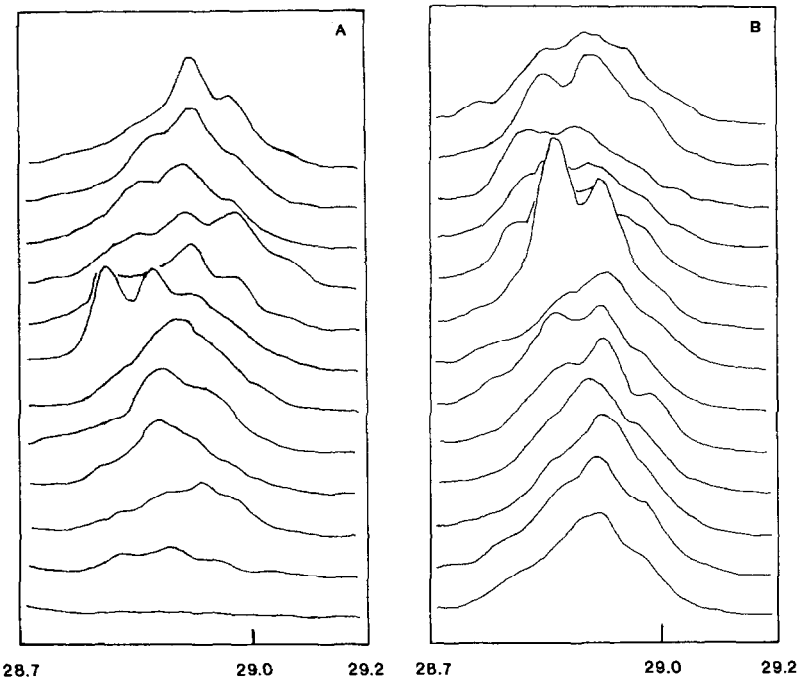

FIG. 1. Splitting of the orthorhombic (111) profile at 595°C in air. The lowermost scan in A begins 1.3 min after temperature is reached. The scans are 4 min apart. At the fifth scan in B, transformation is 90%.

bic phase transformation in PbO. We observed *in situ* that diffraction lines in both phases are split into four to seven peaks during the transformation. The intensities of the peaks fluctuate faster than the scan repetition rate over the 2θ region (Figs. 1 and 2).

2. Experimental

Tetragonal PbO was prepared in our laboratory by the dehydration of wet lead hydroxide by hot 15 *N* KOH. The solution was cooled overnight to allow slow digestion, giving a coarse but well-crystallized product. The powder was gently ground by hand under 100% ethanol. X-ray diffraction showed only sharp lines of the tetragonal phase.

The transformation was observed isothermally in air or flowing He near the transition temperature using a Rigaku DMAX/RB rotating anode X-ray diffraction system and a manufacturer-supplied wraparound radiation furnace with a Pt grid sample holder. The X-ray radiation was Cu$K\alpha$ excited at 8000 W. The furnace heat shield served as a Ni filter, but no monochromater was used. The detector was oscillated at a scan rate of 1°/min with 0.01° sampling over a 2θ region that contained a major peak of each phase.

For comparison, specimens were quenched in liquid N_2 from 585°C and a flowing N_2 atmosphere in a three-zone horizontal tube furnace. The PbO was encapsulated in gold tubing and placed and withdrawn from the at-temperature furnace in a thin-walled alumina cylinder drawn manually along the tube. In this way, the gold capsule was spilled directly from the fur-

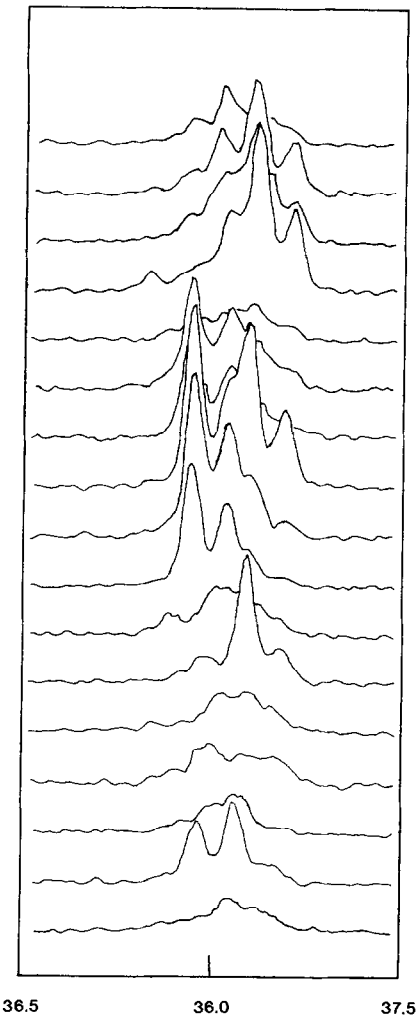

FIG. 2. Splitting of the orthorhombic (020) profile at 587°C in air. The lowermost scan begins 42 min after temperature is reached. The scans are 5 min apart. At the ninth scan, transformation is 90%.

nace into the liquid N_2. Specimens were taken at 15-min intervals.

Diffraction patterns of the quenched specimens were collected with a Rigaku DMAX-IIB X-ray diffractometer with monochromated Cu$K\alpha$ radiation by step scanning at 0.02° sampling with a 2-sec dwell. Five scans were summed, giving a maximum intensity greater than 15-K counts.

3. Results and Discussion

High-temperature X-ray diffraction profiles are shown as a function of time in Figs. 1 and 2. The α_2 component and the background have not been removed, but the profiles were smoothed. The time is increasing from the bottom of the figures to the top.

The (*hkl*) profiles for both phases are split into several lines, each of variable intensity suggesting multiple unit cell distortions.

All quenched specimens show no other phases than the tetragonal and orthorhombic PbO. All profiles are sharp and show no specimen-dependent asymmetries. The integrated intensities give smooth isothermal transformation curves. Any splitting of the profiles is a high-temperature phenomena and is not readily quenchable at these cooling rates.

For the high-temperature diffraction data, rather than a continuous change in *d* spacings there are discrete values for profiles with widths near that of the instrument profile (Fig. 3 shows the *d* spacings as functions of time. The *d* spacings averaged over time for given experiments are tabulated in Tables I and II). The intensities of each peak increase and then decrease continuously without a readily apparent correlation between peaks. However, for some specimens there do appear to be sets of peaks; e.g., in Fig. 1, the $(111)_0$ seems to consist of two sets. This behavior is present for all temperatures, in both air and flowing He, and continues after there is no net change in the percentage of transformation. Although the peaks farthest from the center of the undistorted profile usually have the smallest intensities, this is not consistent and for some scans they may have the greatest intensity. When higher diffraction orders are examined, the splitting is still seen, but the noise level is such that values of the *d* spacings are not reliable and fewer peaks are seen. For the tetragonal phase, the splitting

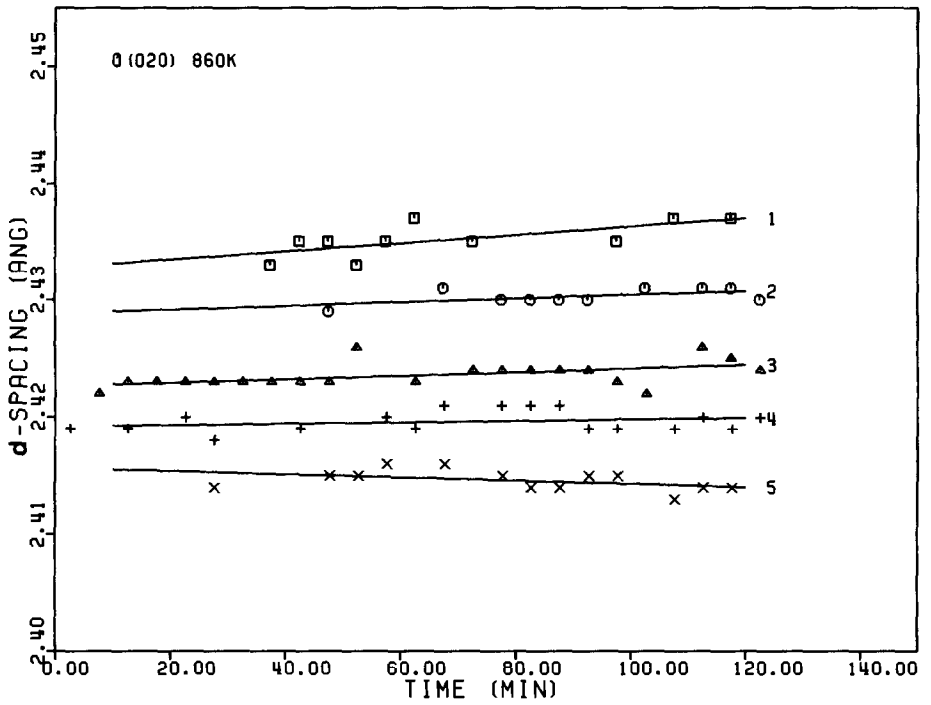

FIG. 3. The d spacings as functions of time for the split $(020)_0$ profile at 587°C in air.

of the profiles is usually not apparent until after ~50% transformation, although the profiles may have a "punched" appearance; the undistorted unit cell dominates the tetragonal diffraction pattern. However, although this peak is always of large relative intensity, it does not dominate the pattern at larger percentage transformations.

The undistorted tetragonal d spacings are the unweighted average of the d spacings of the split profiles. For the tetragonal phase, the average is 3.140 ± 0.016 Å for $(101)_t$ in He and 3.139 ± 0.016 Å in air, and 2.541 ± 0.007 Å for $(002)_t$ in air. Likewise, for the orthorhombic phase, the average is always within 0.001 Å of the center peak of the split profile. Averaged over the specimen, there is no change in symmetry; i.e., the specimen distortion is local rather than global. However, since the profiles are narrow, distortion is over a diffraction domain, which is a region of 1000 Å or more. The splitting is not from a localized strain within a diffraction domain.

An examination of the figures shows that the intensities grow in, then collapse almost catastrophically over the entire 2θ region. When two 2θ regions are observed during a given experiment, the collapse occurs in both. The frequency of the collapse is variable.

Broadening of the individual profiles is evident as they dissolve into the background suggesting (1) a continuous range of d spacings about each peak as one distorted unit cell changes into another or reverts to the opposite phase, (2) a change in the diffraction domain size distribution at the expense of the opposing phase (a shift in the transformation interface), and (3) strain as one diffraction domain infringes or retreats from another at the interface.

The integrated intensities of each set of profiles are not constant, nor do they follow a defined transformation curve (Fig. 4). The

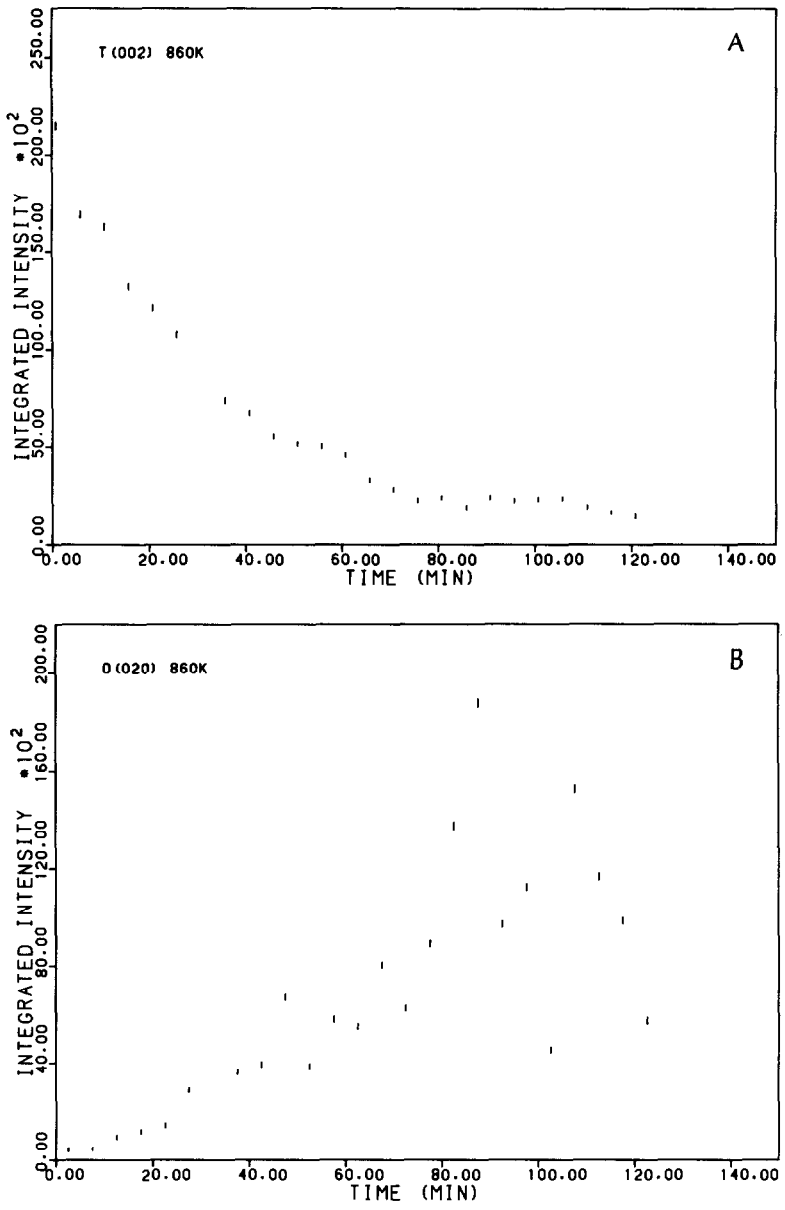

FIG. 4. Integrated intensities as functions of time for the $(002)_t$ profile (A) and the $(020)_0$ profile (B) for the tetragonal ⇄ orthorhombic transformation at 587°C in air. The error bars are determined from Eq. (1).

error bars in Fig. 4 are defined through the relation

$$E = \pm \frac{(N_T + N_B)^{1/2}}{N_T - N_B} N_p, \qquad (1)$$

where $E = \pm\sigma_p N_p$, and N_p, N_B, and N_T are the integrated intensities of the profile, the background, and the profile without removal of the background, respectively, and σ_p is the absolute standard deviation in

TABLE I

THE *d* SPACINGS (Å) FOR THE TETRAGONAL (*hkl*) PROFILES AS AVERAGED OVER THE DURATION OF THE PHASE TRANSFORMATION FOR THE DATA COLLECTED AT A GIVEN TEMPERATURE IN He OR AIR

$(101)_t$		$(002)_t$
580°C, He	595°C, air	587°C, air
3.167	3.168	2.553
3.158	3.156	2.544
3.149	3.148	2.541
3.140	3.139	2.536
3.134	3.134	2.532
3.129	3.129	
3.123	3.124	
3.118	3.117	

Note. The standard deviation of each value is usually less than 0.005 Å.

the net profile integrated intensity (*5*). A smooth transformation curve is expected for *in situ* diffraction at these incident X-ray intensities (*6*). The general trend is to increase irregularly to the final percentage transformation, then vary erratically from scan to scan within 2 to 3 min time. For $(111)_0$ at 595°C the integrated intensities vary as much as 80% of the maximum; the relative peak intensities vary similarly. The measured integrated intensities of each of the phases do not always correspond. For example, at 587°C, Fig. 2, at ~50% transformation as measured by PbO_t, the transformation as measured by PbO_o is ~25%. During a variation in integrated intensity, there is no corresponding variation in the opposing phase. The background is constant within the statistical fluctuations. Although a limited 2θ region was scanned (25° to 40°, 43.6° to 45.6°, and 57.9° to 59.9°), no lines from a third phase are present. Therefore, a crystalline or amorphous phase cannot account for the loss in integrated intensity. A substantial amount of intensity may be lost in the tails from profile broadening, but not to the extent required. The significant "loss" is the shifting of intensity of one line from a distorted unit cell to another at time scales smaller than the measurement repetition rates. This supports the interpretation that the unit cell is undergoing distortions, rather than that PbO reverting to a lower symmetry phase as a transformation intermediate.

TABLE II

THE *d* SPACINGS (Å) FOR THE ORTHORHOMBIC (*hkl*) PROFILES AS AVERAGED OVER THE DURATION OF THE PHASE TRANSFORMATION FOR THE DATA COLLECTED AT A GIVEN TEMPERATURE IN He OR AIR

$(111)_0$		$(020)_0$
580°C, He	595°C, air	587°C, air
3.109	3.105	2.437
3.101	3.096	2.432
3.093	—	2.426
3.089	3.089	2.422
3.085	3.084	2.417
3.077	3.079	
3.073	3.072	
3.118	3.117	

Note. The standard deviation of each value is usually less than 0.005 Å.

The unit cell multiple distortions are not related to an anomalous anisotropic thermal expansion coefficient as discrete *d* spacings are seen and are consistent over a temperature range of Δ15°C; however, the temperature variations from the controller may act as the driving force for a process of low activation energy.

Near-surface *d* spacing fluctuations have been invoked to account for X-ray diffraction profile longitudinal broadening just above T_m in the low-temperature cubic → tetragonal martensitic transformation in V_3Si (*7*, *8*), a high T_c superconductor with the A-15 structure. The fluctuations were considered percursive to the transforma-

tion and were attributed to the lattice instabilities accompanying the soft mode.

However, the lead oxide transformation is for a very different structural phase transition. From symmetry considerations, it is not expected that mode softening is involved in the transformation: the orthorhombic high-temperature phase, having a lower symmetry than the low-temperature phase, would have an order parameter equal to one. Also, the large displacements of the atoms are more consistent with a reconstructive transformation (rather than, for example, a displacive transformation in a titanate, for which atomic displacements are $\lesssim 0.1$ Å).

Oxygen nonstoichiometry may lead to disordering and unit cell distortions. Between 350 to 400°C, PbO reacts with O_2 to form several oxides; however, above 400°C, the oxides decompose to PbO once again; this argument is weakened further in that the fluctuations are also seen in a He atmosphere. PbO discoloration has been affected by production of F centers and the formation of Pb and O_2 by X-ray and photoirradiation (*9*); again, ordering of the defects may lead to distorted unit cells. However, a driving force of the oscillations is necessary; as mentioned above it may be the variable temperature ramp from the controller. But we also suggest a dynamic equilibrium, for which the strain of impinging domains is a function of time as the interface translates. Such a dynamic equilibrium may be nucleation and growth of one phase transforming into the other (*10*) or of recrystallization (*2*). Each diffraction domain of a phase is under compression or extension as "bubbles" of the other phase, or the recrystallized phase, nucleate and grow.

4. Conclusion

High-temperature X-ray diffraction shows a splitting of the diffraction profiles from multiple unit cell distortions. A unit cell distortion extends over the entire diffraction domain, but there is no global change in the specimen symmetry. The origin of the splitting and the intensity fluctuations of each peak is uncertain; it may be from a dynamic equilibrium at the interfaces and of the transformation mechanism or from the presence of ordered defects.

Acknowledgments

The rotating anode x-ray data were obtained on equipment purchased with the NSF Grant No. DMR-9406823. We thank Dr. David Wright of the A.S.U. Center for Solid State Science Materials Preparation Facility for his help in preparing the quenched specimens.

References

1. R. Söderquest and B. Dickens, *J. Phys. Chem. Solids* **28,** 823 (1967).
2. J. R. Schoonover, T. L. Groy, and S. H. Lin, to be published.
3. J. Morales, J. L. Tirado, M. Macius, and A. Ortega, *React. Solids* **1,** 43 (1985).
4. Y. Okuri and Y. Ogo, *Bull. Chem. Soc. Japan* **55,** 3641 (1982).
5. H. P. Klug and L. E. Alexander, "X-Ray Diffraction Procedures," 2nd ed., Wiley, New York (1974).
6. J. R. Schoonover and S. H. Lin, *Mater. Lett.* **7,** 274 (1988).
7. J. B. Hastings, G. Shirane, and S. J. Williamson, *Phys. Rev. Lett.* **43,** 1249 (1979).
8. J. B. Hastings, Y. Fujii, G. Shirane, and S. J. Williamson, *Phys. Rev. B* **28,** 322 (1983).
9. M. S. Kosman and V. A. Izvozchikov, *Fiz. Tverd. Tela (Leningrad)* **3,** 119 (1961).
10. T. L. Groy, S. H. Lin, S. K. Porter, R. B. Von Dreele, and L. Eyring, *J. Mol. Sci.* **2,** 93 (1982).